

## Transition to spatiotemporal chaos in the damped Kuramoto-Sivashinsky equation

K. R. Elder,<sup>1,2</sup> J. D. Gunton,<sup>3</sup> and Nigel Goldenfeld<sup>2</sup>

<sup>1</sup>*Department of Physics, Oakland University, Rochester, Michigan 48309-4401*

<sup>2</sup>*Department of Physics and Materials Research Laboratory, University of Illinois at Urbana-Champaign, 1110 West Green Street, Urbana, Illinois 61801-3080*

<sup>3</sup>*Department of Physics, Lehigh University, 16 Memorial Drive East, Bethlehem, Pennsylvania 18015-3182*

(Received 23 May 1996; revised manuscript received 12 May 1997)

The transition from a lamellar or periodic state to spatiotemporal chaos was examined numerically in the damped Kuramoto-Sivashinsky equation. The behavior of several quantities was examined near the transition as the system size was doubled five times and no systematic changes were observed. Thus there was no evidence to support a divergence at the transition in the infinite system size limit. This provides strong evidence of a discontinuous transition. [S1063-651X(97)11908-0]

PACS number(s): 05.45.+b, 47.20.Lz, 64.60-i

Spatiotemporal chaos is a complex phenomena that arises in many driven nonequilibrium systems such as directional solidification [1–3], Rayleigh-Bénard convection [4,5], parametrically driven surface waves [6], electroconvection [7] and directional viscous fingering [8]. These examples illustrate the ubiquitous and diverse nature of spatiotemporal chaos. The purpose of this paper is to provide an accurate description of the transition from an ordered regular (or lamellar) state to spatiotemporal chaos for the specific case of the damped Kuramoto-Sivashinsky equation [9–13]. Several attempts [10–12] have been made to understand the order of this transition, but have led to somewhat ambiguous results. To provide a more definitive description, the behavior of the system was analyzed as a function of system size. The results of these calculations show no systematic changes near the transition as the system size was doubled five times, providing strong evidence of a discontinuous or first-order transition. Furthermore the simulations indicate that the transition is initiated by an instability to breathing modes.

In many driven nonequilibrium systems, primary instabilities generate periodic patterns that become unstable to secondary instabilities which generate chaotic or disordered structures. A classic example of this is in directional solidification [1–3,9,14–17] in which a liquid-solid system is driven through a temperature gradient at constant velocity such that the liquid is continuously converted to a solid. If solidification is accompanied by impurity rejection, the buildup of impurities at the interface can lead to a primary instability known as the Mullins-Sekerka [14,15] instability. At small pulling velocities this tends to select a periodic cellular interface with characteristic wavelength  $\lambda$ . At some critical driving force, experiments [1,16] and theoretical work [2,3,17] have shown that secondary instabilities generate dynamical behavior, such as breathing and solitary modes and birth and death sequences, which can give rise to patterns that are disordered in both space and time as observed in experiment [1]. For systems with a large aspect ratio (i.e.,  $\mathcal{L}/\lambda \gg 1$ , where  $\mathcal{L}$  is the system width) this behavior is referred to as spatiotemporal chaos [11] or weak turbulence. While this novel behavior occurs in a wide variety of systems [18], the nature of the chaotic states and the transition to these states can take many forms.

In the case of the one-dimensional complex Ginzburg-Landau model, for example, it is known that one can have phase defect chaos, in which the amplitude of the complex order parameter vanishes at a finite density of points, and where the phase can slip by a multiple of  $2\pi$ . Numerical studies also suggested [19] that there was phase chaos (phase turbulence), which is a chaotic state defined by the absence of defects. This study also reported that there were continuous and discontinuous transition lines separating phase defect chaos and phase chaos states. However, more recent simulations on larger systems show that the continuous transition is more accurately described as a smooth crossover rather than a sharp transition, and suggest that phase chaos might not exist in the thermodynamic limit [20,21]. The transition studied in this paper is from an ordered periodic structure to spatiotemporal chaos, and thus is distinctly different from such chaos-chaos transitions. Reviews of other examples of spatiotemporal chaotic states and corresponding transitions are given in Refs. [22] and [23] for the two-dimensional complex Ginzburg-Landau model and coupled map lattice models, respectively. The one-dimensional coupled map lattice models studied by Chaté and Manneville [24] and others are perhaps more relevant to this work, as the maps described a transition from lamellar states to spatiotemporal chaos. The numerical work on these models suggest a continuous transition.

The damped Kuramoto-Sivashinsky equation provides a crude model of directional solidification that encompasses the generic behavior described earlier (i.e., at small driving forces a primary instability leads to stationary periodic or lamellar patterns, while at large driving forces secondary instabilities generate spatiotemporal chaos). Additionally, many of the secondary instabilities that appear in the damped Kuramoto-Sivashinsky equation, such as breathing and solitary modes, birth and death sequences, and tip splitting, have been observed in directional solidification experiments [1,16]. The purpose of this paper is to use the damped Kuramoto-Sivashinsky equation to examine the transition from periodic stationary states to spatiotemporal chaos. It is hoped that the results of these calculations will be relevant to real directional solidification and other similar one-dimensional driven interfaces.

The damped Kuramoto-Sivashinsky equation can be written

$$\partial_t \psi = [r - (1 + \partial_{xx})^2] \psi - \psi \partial_x \psi, \quad (1)$$

where  $r$  is a control parameter related to the driving force. To the limited extent that this equation models directional solidification,  $\psi$  can be interpreted as the interfacial position,  $x$  is the distance along the interface, and  $t$  is time. The primary instability to forming periodic structures can be easily be obtained by a linear analysis which gives  $\hat{\psi}(q, t) = e^{\sigma(q)t} \hat{\psi}(q, 0)$ , where  $\hat{\psi}(q, t) = \int dx e^{ikx} \psi(x, t)$  and  $\sigma(q) = r - (1 - q^2)^2$ . Thus Fourier modes in the region  $\sqrt{1 - \sqrt{r}} < q < \sqrt{1 + \sqrt{r}}$  are linearly unstable, and the most unstable mode is at  $q = 1$ . This primary instability leads to a family of stationary periodic solutions, which exist in the region bounded by  $(1 - q_o^2)^2 < r < (1 - 4q_o^2)^2$ , where the stationary solutions are written in the form  $\psi = \sum a_n \sin(nq_o x)$ .

The stationary solutions are dynamically unstable near the upper and lower boundaries. These instabilities are known as secondary instabilities, and were described by Misbah and Valence [13]. The particular solutions that are selected are dependent on both the aspect ratio and initial conditions. The present work focuses mainly on the behavior of Eq. (1) in the large aspect ratio limit with a random initial condition. For these conditions a lamellar state is selected for small  $r$ , while, for large  $r$ , secondary instabilities appear and lead to the disordered state that is characteristic of spatiotemporal chaos. The critical value of  $r$  at which the transition to spatiotemporal chaos occurs is at  $r_c \approx 0.688$  [10]. The disordered and lamellar states are respectively characterized by correlations that decay exponentially in space and time and by large (i.e., of the order of the system size) ordered periodic or lamellar regions. Some discussion of other initial conditions is given in Ref. [11].

The first numerical investigation of the transition in the damped Kuramoto-Sivashinsky equation was conducted by Chaté and Manneville [10] in 1987. An interesting transient behavior was observed, in which well-defined disordered and lamellar regions coexist. It was found that the disordered-lamellar front moves at a constant velocity such that the disordered regime invades the lamellar phase above the transition and recedes below. The front velocity was found to go continuously to zero at the transition. This continuous change in the front velocity was interpreted as an indication of a continuous transition. In support of this interpretation, the distribution of lamellar domains was shown to be nonexponential at the transition. The behavior of the front velocity is, however, consistent with a standard first-order or discontinuous transition. For example, in a liquid-solid transition the velocity of a liquid-solid front is proportional to the undercooling and continuously goes to zero at the melting transition. In addition it is not obvious that an exponential distribution should occur exactly at a discontinuous transition in a one-dimensional system. At the transition it is very difficult for one state to dominate, since in one dimension the velocity of the domain walls is exactly zero and there are no curvature effects to eliminate small domains. Thus it is easy for the system to get stuck in metastable states that would not necessarily have exponential distributions. More recent discussions of the damped Kuramoto-Sivashinsky equation by

Manneville [11] admit the possibility of a discontinuous or at least weakly first-order transition. In this regard, it is worth noting that Chaté and Manneville originally reported [10] the Hopf bifurcation to be subcritical. This makes a discontinuous transition to spatiotemporal chaos more likely than if the Hopf bifurcation had been supercritical.

Numerical simulations conducted in 1995 [12] found discontinuities in all quantities that were considered at the transition. Nevertheless, as the transition was approached from above, many quantities, such as the average lamellar domain size, increased. This behavior is consistent with a continuous transition in a finite-size system. In a continuous transition these quantities should diverge with system size as  $r_c$  is approached. To examine this possibility, simulations of Eq. (1) were conducted on a system of size  $\mathcal{L} = 536$ . The results of this simulation were then compared with successively larger systems of sizes  $\mathcal{L} = 1072, 2145, 4289, \text{ and } 8579$ . The five systems considered have aspect ratios of approximately 80, 160, 320, 640, and 1280.

The damped Kuramoto-Sivashinsky equation was simulated using a standard forward-Euler scheme for the time derivative and central difference formulas for the spatial derivatives. A relatively large time step ( $dt = 0.01$ ) and mesh size ( $dx = \pi/6$ ) were chosen in an attempt to study the late time large wavelength behavior of the equation. Although the convergence of the solutions to the continuum limits was not examined, the numerical solutions did contain the same instabilities as detected in other work [13], although the parameter ranges over which the various solutions occur are slightly altered. For example the transition from periodic to disordered solutions occurs at roughly  $r \approx 0.635$  for the numerical algorithm, while it occurs at  $r \approx 0.68$  for the continuum model.

To provide a detailed description of the transition, the power spectrum or structure factor was determined as a function of  $r$ . The structure factor is defined to be

$$S(q) \equiv \langle |\hat{\psi}_q|^2 \rangle, \quad (2)$$

where

$$\hat{\psi}_q \equiv N^{-1} \sum_{j=1}^{j=N} e^{ijdx} \psi_j, \quad (3)$$

the brackets ( $\langle \rangle$ ) refer to an average over 100 runs,  $q = 2\pi k/Ndx$ , and  $N$  is the number of spatial grid points used. A sample structure factor is shown in Fig. 1. This spectrum can be characterized by a correlation length  $\zeta$ , peak height  $S_p$ , and peak position  $q_p$ , as shown in Fig. 1. The correlation length in this instance is a measure of the average size of lamellar domains, and should diverge for a continuous transition.

At very large  $r$ , the system rapidly relaxes to a state characterized by a broad  $S(k)$ . As  $r$  decreases, the correlation length and peak height increase. To determine whether these quantities diverge as  $r$  approaches  $r_c$ , five different system sizes were examined (i.e.,  $N = 2^{10}, 2^{11}, 2^{12}, 2^{13}, \text{ and } 2^{14}$ ). In Fig. 1,  $S(k)$  is shown for three different system sizes just above  $r_c$ . This figure shows that the power spectrum for the different system sizes are statistically indistinguishable at  $r = 0.64$ . Similar results are obtained for all values of  $r$  above

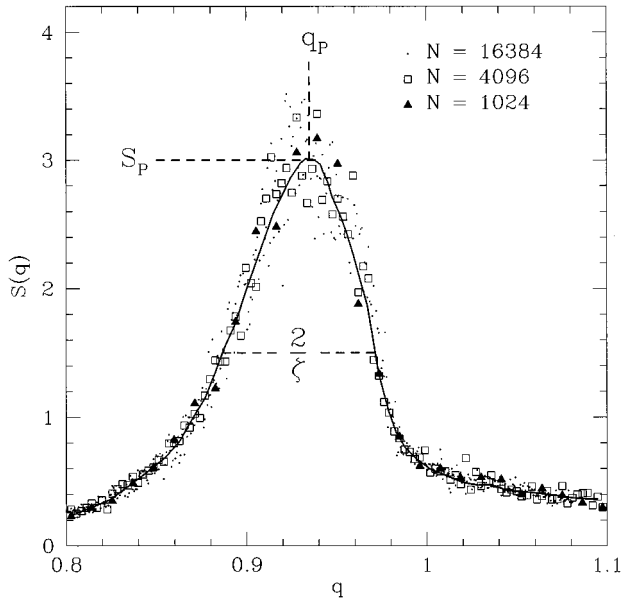


FIG. 1. Power spectrum at  $r=0.64$ , for systems of sizes  $N=2^{10}$ ,  $2^{12}$ , and  $2^{14}$ . The solid line is a guide to the eye.

$r_c$ . To illustrate this point, the peak height and correlation length were determined as a function of  $r$  for five different system sizes. The results of these calculations are displayed in Fig. 2. A finite-size scaling analysis of the data was attempted by fitting the numerical results to a scaling relationship of the form  $\zeta = \mathcal{L}^\beta \mathcal{F}[(r-r_c)^\alpha/\mathcal{L}]$ . The analysis is somewhat trivial in that no variation of  $\zeta$  with  $\mathcal{L}$  was found, consistent with an exponent of  $\beta=0$ . The quality of the data could not lead to a more precise conclusion. Thus there was no evidence that the correlation length would diverge as  $r \rightarrow r_c$  in the infinite system size limit. This is very strong evidence that the transition is discontinuous.

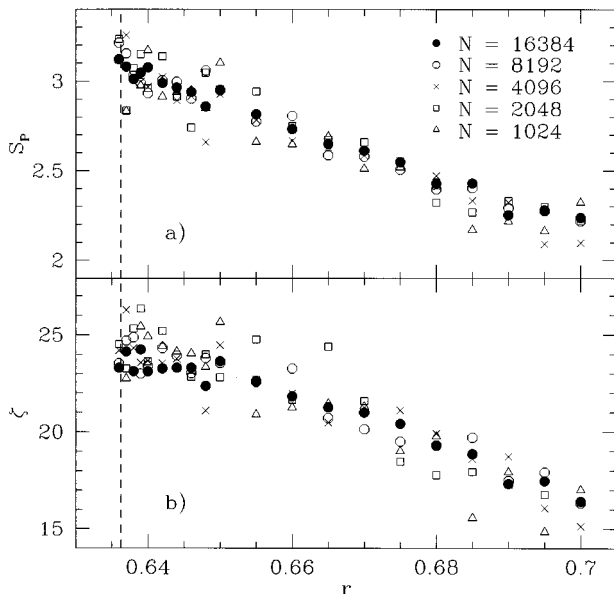


FIG. 2. Finite-size scaling analysis of the correlation length ( $\zeta$ ) and peak height of  $S(q)$  ( $S_P$ ). In both (a) and (b) systems from  $N=2^{10}$  to  $N=2^{14}$  are examined.

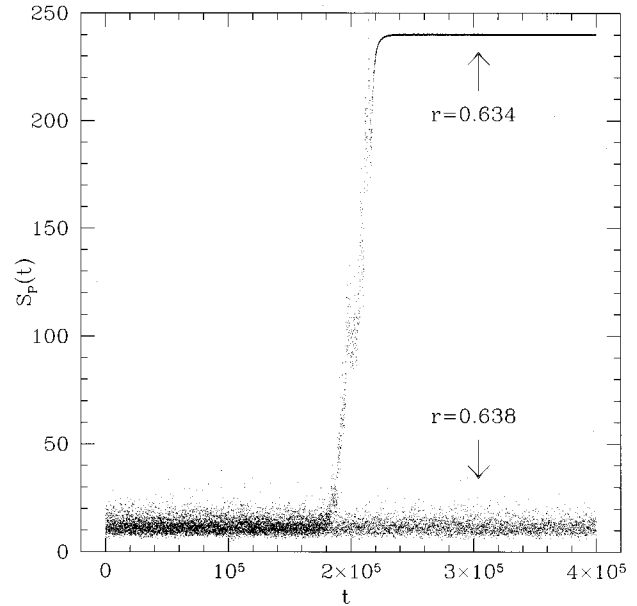


FIG. 3. Dynamics of peak height for  $r=0.634$  and  $0.638$ .

For  $r$  very close to but below  $r_c$ , the system first relaxes to a disordered state, that is characterized by a power spectrum very similar to that shown in Fig. 1. However, this is a “metastable” state that will eventually “nucleate” periodic regimes. An example of such a nucleation event is shown in Fig. 3. In this figure  $S_P$  is displayed for a single run for two values of  $r$ , one just above  $r_c$  (i.e.,  $r=0.638$ ) and one just below (i.e.,  $r=0.634$ ). At early times these systems are more or less indistinguishable, but at later times the system just below  $r_c$  nucleates an ordered periodic regime. For values of  $r$  very close to the transition, it is possible to obtain a coexistence of periodic and chaotic regimes for long time periods. It is also possible to nucleate a disordered state above  $r_c$  if the system is initially prepared in the lamellar state. In fact if  $r$  is ramped through the transition, hysteresis loops can be obtained [11]. All these observations are consistent with a discontinuous phase transition.

As the transition is crossed, there is a sharp jump in the value of all measured quantities. This was observed in previous studies of a single system size [12]. To understand this transition it is useful to consider the jump in the peak wave vector ( $q_P$ ). This is shown in Fig. 4. The dashed line in this figure corresponds to the boundary above which periodic solutions are dynamically unstable to breathing modes for the numerical algorithm used in this work. As the transition is approached there is a discontinuous jump in  $q_P$  at  $r_c \approx 0.6375$  such that  $q_P$  is to the left of the breathing mode boundary for  $r > r_c$  and to the right for  $r < r_c$ . Thus it is apparent that the transition coincides with the appearance of breathing modes.

In summary, the results of the numerical analysis of the damped Kuramoto-Sivashinsky equation indicate that the transition from an ordered lamellar state to spatiotemporal chaos is discontinuous. Furthermore, it is shown that the onset of spatiotemporal chaos is coincident with the appearance of the breathing modes. While this work cannot identify cause and effect, it is tempting to speculate that the selection of breathing modes leads to spatiotemporal chaos.

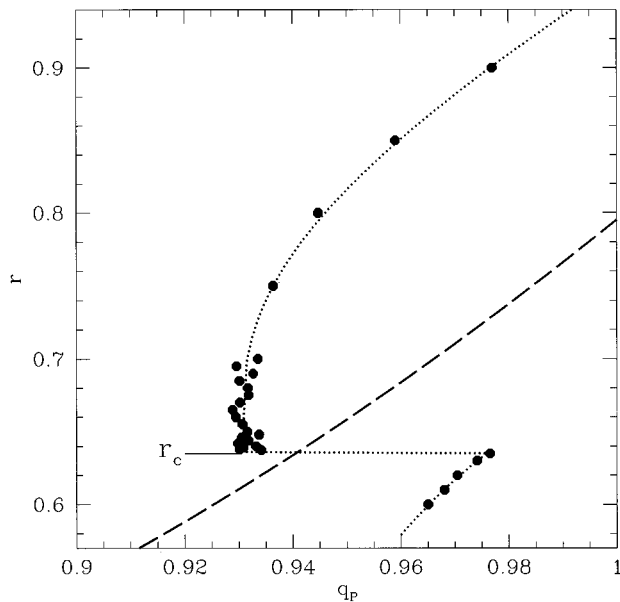


FIG. 4. Selected wave vector. The solid points correspond to the peak wave vector selected for a given  $r$ . The dashed line defines the boundary between stable and unstable stationary periodic solutions. Above this line the stationary solutions are dynamically unstable to a secondary instability that gives rise to breathing modes. The dotted line is a guide to the eye.

The results of this research should be applicable to other one-dimensional front propagation phenomena such as directional solidification and viscous fingering. It is, however, important to note that the nature of the transition can be quite

different in other systems. It is also likely that dimension will play an important role in determining the nature of the transition as occurs in equilibrium systems. An interesting two-dimensional example is parametrically driven surface waves [6]. In this system at small driving forces a primary instability (the Faraday instability) produces spatially periodic structures, while at larger driving forces a secondary instability appears (i.e., a transverse amplitude modulation) that does not break the lamellar order. At very large driving forces spatiotemporal chaos does appear. This transition to spatiotemporal chaos most likely arises when the amplitude of the transverse amplitude modulations becomes of the order of the wavelength of the original periodic structures. A very similar behavior was observed in recent simulations of the two-dimensional damped Kuramoto-Sivashinsky equation [25], in which a well-ordered breathing state appeared at intermediate driving forces. Although the results of these simulations were not conclusive, the transition from the breathing state to spatiotemporal chaos was consistent with a continuous transition. Thus the nature of the transition appears to be different in two dimensions.

KRE would like to thank Martin Tarlie, Marco Paniconi, and Haowen Xi for many useful discussions. This work was supported by the following grants: Grant No. NSF-DMR-8920538 administered through the University of Illinois Materials Research Laboratory and Research Corporation Grant No. CC4181 (K.R.E.); Grant No. NSF-DMR-9596202 (J.D.G.); and Grant No. NSF-DMR-93-14938 (N.G.). We would also like to acknowledge the support of the Pittsburgh Supercomputing Center.

- 
- [1] J. T. C. Lee, K. Tsiveriotis, and R. A. Brown, *J. Cryst. Growth* **121**, 536 (1992).
- [2] M. J. Bennett, K. Tsiveriotis, and R. A. Brown, *Phys. Rev. B* **45**, 9562 (1992).
- [3] A. Valance, K. Kassner, and C. Misbah, *Phys. Rev. Lett.* **69**, 1544 (1992).
- [4] S. W. Morris, E. Bodenschatz, D. S. Cannell, and G. Ahlers, *Phys. Rev. Lett.* **71**, 2026 (1993).
- [5] H. W. Xi, J. D. Gunton, and J. Viñals, *Phys. Rev. Lett.* **71**, 2030 (1993); *Phys. Rev. E* **47**, R2987 (1993).
- [6] W. Zhang and J. Viñals, *Phys. Rev. Lett.* **74**, 690 (1995).
- [7] M. Dennin, G. Ahlers, and D. S. Cannell, *Science* **272**, 388 (1996).
- [8] Y. Couder, S. Michalland, M. Rabaud, and H. Thomé, in *Nonlinear Evolution of Spatio-Temporal Structures in Dissipative Continuous Systems*, Vol. 225 of *Nato Advanced Study Institute Series B: Physics*, edited by F. H. Busse and L. Kramer (Plenum, New York, 1990), p. 487.
- [9] A. Novick-Cohen and G. I. Sivashinsky, *Physica D* **20**, 237 (1986).
- [10] H. Chaté and P. Manneville, *Phys. Rev. Lett.* **58**, 112 (1987).
- [11] P. Manneville, *Dissipative Structures and Weak Turbulence* (Academic, New York, 1990).
- [12] K. R. Elder, Hao-wen Xi, Matt Deans, and J. D. Gunton, in *Proceedings of the CAM-94 Physics Meeting, Cancun, Mexico, 1994*, edited by Arnulfo Zepeda, AIP Conf. Proc. No. 342 (AIP, New York, 1995).
- [13] C. Misbah and A. Valance, *Phys. Rev. E* **49**, 166 (1994).
- [14] W. W. Mullins and R. F. Sekerka, *J. Appl. Phys.* **35**, 444 (1964).
- [15] J. S. Langer, *Rev. Mod. Phys.* **52**, 1 (1980).
- [16] J. -M. Flesselles, A. J. Simon, and A. J. Libchaber, *Adv. Phys.* **40**, 1 (1991), and references therein.
- [17] B. Grossmann, K. R. Elder, M. Grant, and J. M. Kosterlitz, *Phys. Rev. Lett.* **71**, 3323 (1993).
- [18] M. C. Cross and P. C. Hohenberg, *Rev. Mod. Phys.* **65**, 851 (1993) and references therein.
- [19] B. I. Shraiman, A. Pumir, W. Van Saarloos, P. C. Hohenberg, H. Chaté, and M. Hohenberg, *Physica D* **57**, 241 (1992).
- [20] D. A. Egolf and H. S. Greenside, *Nature (London)* **369**, 129 (1994).
- [21] D. A. Egolf and H. S. Greenside, *Phys. Rev. Lett.* **74**, 1751 (1995).
- [22] H. Chaté and P. Manneville, *Physica A* **224**, 348 (1996).
- [23] H. Chaté and P. Manneville, *Prog. Theor. Phys.* **87**, 1 (1992).
- [24] H. Chaté and P. Manneville, *Physica D* **32**, 409 (1988).
- [25] M. Paniconi and K. R. Elder, *Phys. Rev. E* (to be published).